Astron. Astrophys. 317, 742–748 (1997)

ASTRONOMY AND ASTROPHYSICS

Line-profile variations of non-radial adiabatic pulsations of rotating stars

III. On the alleged misidentification of tesseral modes

J.H. Telting and C. Schrijvers

Astronomical Institute Anton Pannekoek, University of Amsterdam, and Center for High Energy Astrophysics, Kruislaan 403, 1098 SJ Amsterdam, Netherlands

Received 22 March 1996 / Accepted 3 June 1996

Abstract. We use a model of a non-radially, adiabatically pulsating rotating star to generate time series of absorption line profiles. We analyse the spectral time series of a tesseral mode with pulsation parameters ℓ=2 and m=−1, to obtain amplitude and phase diagrams as a function of position in the line profile. We investigate whether the phase diagrams can be used to identify the pulsation parameters ℓ and $|m|$ of this mode.

As opposed to the findings of Reid & Aerts (1993), we find that the effects of the Coriolis force do not hinder the identification of the degree ℓ of the pulsation mode, but that the exact value of i=90° that they used does. We show that for an inclination angle just slightly different from 90° the chances for an erroneous identification of the degree ℓ of the ℓ=2, m=−1 pulsation mode, by means of a spectroscopical phase diagram, are very small.

We also discuss the interpretation of observed line-profile variations in the Be star η Cen, where a tesseral mode with ℓ=7 and m=|6| might be present.

Key words: stars: early-type, oscillations, rotation – line: profiles – stars individual: η Cen

1. Introduction

Many early-type stars are known to be pulsating in modes other than radial. The non-radial pulsations divide the stellar surface in regions with different velocity fields, which, in the presence of rotation, redistribute the flux over the absorption line profile to create moving patterns of peaks and troughs. These features cross the profile from blue to red on a time scale of hours to days. Such line-profile changes have been observed, and successfully modelled as the result of non-radial pulsations (e.g., Smith 1978, Vogt & Penrod 1983, Baade 1984, Gies & Kullavanijaya 1988, Kambe et al. 1990, Henrichs 1991, Kennelly et al. 1992, Floquet et al. 1992, Reid et al. 1993).

The two most widely studied spectroscopic methods to identify pulsation modes in early-type stars involve a period search on either the variations of the velocity moments of the absorption lines (the moment method, Balona 1986, Aerts et al. 1992, Mathias et al. 1994) or the intensity variations across the line profiles (Gies & Kullavanijaya 1988, Kambe et al. 1990).

With the first technique one looks for periodicity in the change of derived quantities (moments), such as equivalent width (M_0), apparent radial velocity (M_1), line width (M_2) and skewness (M_3). Mode identifications are obtained by considering the characteristic changes as a function of pulsation phase in each of these quantities.

With the second method (hereafter referred to as the Intensity Period Search, IPS) one searches for periodicity in the normalized intensity of each wavelength bin across the absorption line. For a star with a sufficiently high $V_{\rm e} \sin i$ the pulsational variations of different parts of the stellar surface are Doppler-mapped to distinct parts of the absorption line profile, and the observed change in phase of the periodic variations as a function of wavelength can be used for mode identification. For the few reported mode identifications performed with the IPS method the authors assumed that the detected pulsation modes are sectoral, i.e. ℓ=$|m|$. Telting & Schrijvers (1996, Paper II) showed (1) that this assumption is not necessary, (2) that the absolute phase difference of the intensity variations across the line profile is a good measure of the degree ℓ (rather than the azimuthal order m), and (3) that in some cases the value of $|m|$ can be estimated from the phase difference of the line-profile variations with the first harmonic of the apparent pulsation frequency.

Aerts & Waelkens (1993) discussed the implications of stellar rotation for the velocity field of normal mode eigenfunctions of slowly rotating stars, and in particular the effects on line-profile variations. Reid & Aerts (1993) used the model of Aerts & Waelkens to generate time series of absorption line profiles. They concluded that for the tesseral mode ℓ=2, m=−1 an analysis with the IPS method fails to retrieve the values of the input parameters. They attributed this to a combination of ef-

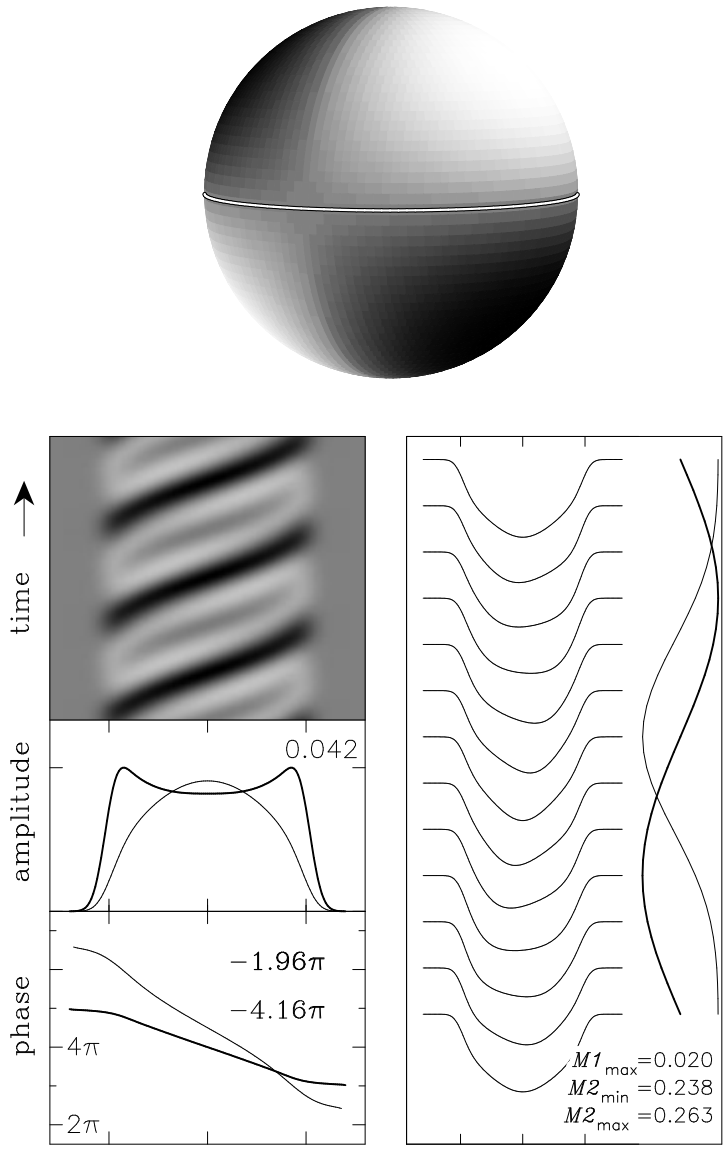

Fig. 1. *Upper* Radial velocity distribution of a normal mode with ℓ=2, $|m|$=1 and i=85°; the equator is indicated by the white line. *Lower* Line-profile variations due to a pulsation mode with ℓ=2, m=−1, and i=85°, $V_e \sin i$=100 km/s, W=15 km/s, $\Omega/\omega^{(0)}$=0.25, $V_{\max}$=27.5 km/s, $k^{(0)}$=0.25. The ticks on the horizontal axes mark $V_e \sin i$. *Right* Line profiles for one complete pulsation cycle, and the variations of the first (thick curve) and second (thin curve) velocity moment. The first moment has an amplitude of 0.02($V_e \sin i$) km/s; the second velocity moment ranges between 0.24 – 0.26($V_e \sin i$)^2 (km/s)^2. Both moments are drawn on scales different from that of the line profiles. *Left* IPS diagnostics: (top) time series of residual spectra with intensity as grey levels; low intensity is coded dark, (middle) distribution of the amplitude of variations across the line profile, with the maximum value in units of average central line depth, (bottom) distribution of phase of variations across the line profile, with the blue-to-red phase difference in radians. Thick curves depict the amplitude and phase distribution $I_0(\lambda)$ and $\Psi_0(\lambda)$, thin curves depict the harmonic amplitude and phase distribution $I_1(\lambda)$ and $\Psi_1(\lambda)$

fects of the chosen value of the inclination, i=90°, and effects of the rotation of the star, and questioned the general applicability of the IPS method.

In this paper we show that the inconsistency as found by Reid & Aerts is entirely due to their choice of an inclination angle exactly equal to 90°, and not due to effects of rotation. Furthermore, we argue that the probability of misinterpreting the degree of the ℓ=2 and m=−1 mode with the IPS method is very small, and hence that the applicability of the method is generally broader than suspected by Aerts & Waelkens (1993).

This paper is part of a series on line-profile variations of non-radially pulsating stars. Schrijvers et al. (1996, Paper I) presented the model that we use in our work, and discussed the effects of rotation and other parameters on the IPS amplitude and phase diagrams. Telting & Schrijvers (1996, Paper II) investigated the general diagnostic value of the phases of variability as a function of wavelength (i.e. the phase diagrams). For other work on line-profile variations due to non-radial pulsations see e.g. Kambe & Osaki (1988), Lee et al. (1992), and Clement (1994).

In Sect. 2 we briefly recall the model of non-radial adiabatic oscillations, and we discuss the analysis of generated time series of spectra in Sect. 3. In Sect. 4 we present the results of our computations and discuss in detail the effects of inclination and rotation on the observable line-profile variations caused by a spheroidal tesseral mode with ℓ=2 and m=−1. We briefly discuss the case of the Be star η Cen in Sect. 5. We give concluding remarks in Sect. 6.

2. Modelling non-radial pulsations of slowly rotating stars

We model line profiles as due to adiabatic non-radial pulsations of a star. We use a model which is essentially the same as the one described by Aerts & Waelkens (1993) but with a few improvements which we discussed in Paper I. The model gives the velocity field for an adiabatic oscillation, as derived

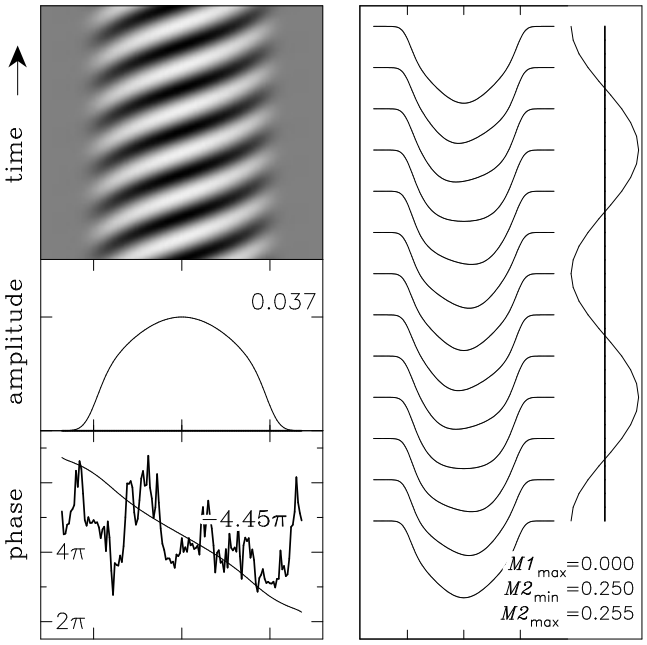

Fig. 2. As Fig. 1, but for i=90°. Note that in this equator-on case the variation of the first moment vanishes for a mode with ℓ=2, $|m|$=1, and that the phase diagram Ψ_0 is undefined since there are no intensity variations with the pulsation frequency. The second moment shows sinusoidal variations with twice the pulsation frequency, i.e. the first harmonic frequency. The amplitude and phase diagram of the intensity variations with the first harmonic frequency ($I_1(\lambda)$, $\Psi_1(\lambda)$) are not very different from that for i=85° (Fig. 1)

from a linear perturbation analysis of the equations of stellar structure, including terms describing the effects of the Coriolis force. From the perturbation analysis it follows that the eigenfunctions of the star can be separated into an angular part with known dependence on the θ and ϕ coordinates, and a radial part containing the pulsation amplitudes which have an unknown radial dependence. The Lagrangian displacement vector at the stellar surface $\boldsymbol{\xi}$=($\xi_r, \xi_\theta, \xi_\phi$) can be expressed as

$$\boldsymbol{\xi} = a_{\mathrm{sph},\ell}\left(1, k\frac{\partial}{\partial\theta}, k\frac{1}{\sin\theta}\frac{\partial}{\partial\phi}\right) N_\ell^m Y_\ell^m(\theta,\phi)\,\mathrm{e}^{\mathrm{i}\omega t}$$
$$+\; a_{\mathrm{tor},\ell+1}\left(0, \frac{1}{\sin\theta}\frac{\partial}{\partial\phi}, -\frac{\partial}{\partial\theta}\right) N_\ell^m Y_{\ell+1}^m(\theta,\phi)\,\mathrm{e}^{\mathrm{i}(\omega t+\frac{\pi}{2})}$$
$$+\; a_{\mathrm{tor},\ell-1}\left(0, \frac{1}{\sin\theta}\frac{\partial}{\partial\phi}, -\frac{\partial}{\partial\theta}\right) N_\ell^m Y_{\ell-1}^m(\theta,\phi)\,\mathrm{e}^{\mathrm{i}(\omega t-\frac{\pi}{2})}\ ,$$

where $a_{\mathrm{sph},\ell}$ is the spheroidal radial amplitude and k is the ratio of horizontal to radial spheroidal amplitudes. The spherical harmonics Y_ℓ^m specify the θ and ϕ dependence of the eigenfunction, and are normalized by the factor N_ℓ^m (see Paper I). In this equation the oscillation frequency ω is defined in the frame that is corotating with the star. The toroidal terms are due to the Coriolis force; the known amplitudes $a_{\mathrm{tor},\ell-1}$ and $a_{\mathrm{tor},\ell+1}$ are proportional to $\Omega/\omega^{(0)}$, with Ω the rotation frequency of the star and $\omega^{(0)}$ the pulsation frequency in the non-rotating case. For a discussion of the limitations of this model we refer to Saio (1981), Martens & Smeyers (1982, 1986), Aerts & Waelkens (1993) and Paper I.

We write the surface value of the ratio of horizontal to radial spheroidal amplitudes as k=$k^{(0)}$+$k^{(1)}\Omega/\omega^{(0)}$ and use the expression for $k^{(1)}$ as given in Paper I. For our study on line-profile characteristics we treat the unknown surface quantities a_{sph} and $k^{(0)}$, the degree ℓ, the azimuthal order m, and the rotation parameter $\Omega/\omega^{(0)}$ as free parameters.

We model the line-profile variations, as seen in the frame of the observer, as a result of the Doppler velocities which are associated with the presence of the oscillatory motions on the surface of the star. We neglect the effects that local temperature and gravity changes might have on the line profiles. The velocity field of the oscillation is found by taking the time derivative of the Lagrangian displacement, and is calculated on a sphere with typically more than 5000 visible equally sized surface elements. Line profiles are then generated by a weighted integration of the Doppler-shifted Gaussian intrinsic profile (with width W, see Paper I) over all visible surface elements. The weights are given by the aspect angle of each element and by a linear limb-darkening correction with α=0.35 (the phase diagrams do not depend on the limb-darkening coefficient α, see Paper I). When computing the aspect angles of the surface elements, we neglect the distortion of the star caused by the displacement field of the pulsation.

3. The analysis of time series of spectra

To investigate the effects of inclination and rotation for the line-profile characteristics of a spheroidal mode with ℓ=2 and $|m|$=1 we generate time series of spectra and analyse these series in a similar way as Reid & Aerts (1993) did, thus creating phase diagrams as a result of the IPS technique. Additionally, we compute the first two velocity moments of the line profiles; the moments are derived by a weighted summation of the normalized intensity $I(V)$ across the line profile

$$M_j \equiv \int (V - V_{\mathrm{ref}})^j (1 - I(V)) dV\ , \qquad (2)$$

where V_{ref} is a reference velocity. The first moment is calculated with the rest wavelength of the line as reference, yielding the radial velocity shift of the line. The second moment is calculated using the first moment as reference velocity V_{ref}, and gives a measure of the squared width of the line. We normalized the velocity moments by dividing each moment by the equivalent width M_0. The relation between our moments (Figs. 1 and 2) and the moments as defined by Aerts et al. (1992) is given in Paper I.

In Fig. 1 we present an example of an analysis of a time series of spectra. We chose the pulsation amplitude such that the maximum surface velocity vector of the pulsation V_{max} = $\left(\sqrt{V_r^2 + V_\theta^2 + V_\phi^2}\right)_{\mathrm{max}}$ equals 27.5 km/s, and we used $k^{(0)}$=0.25,

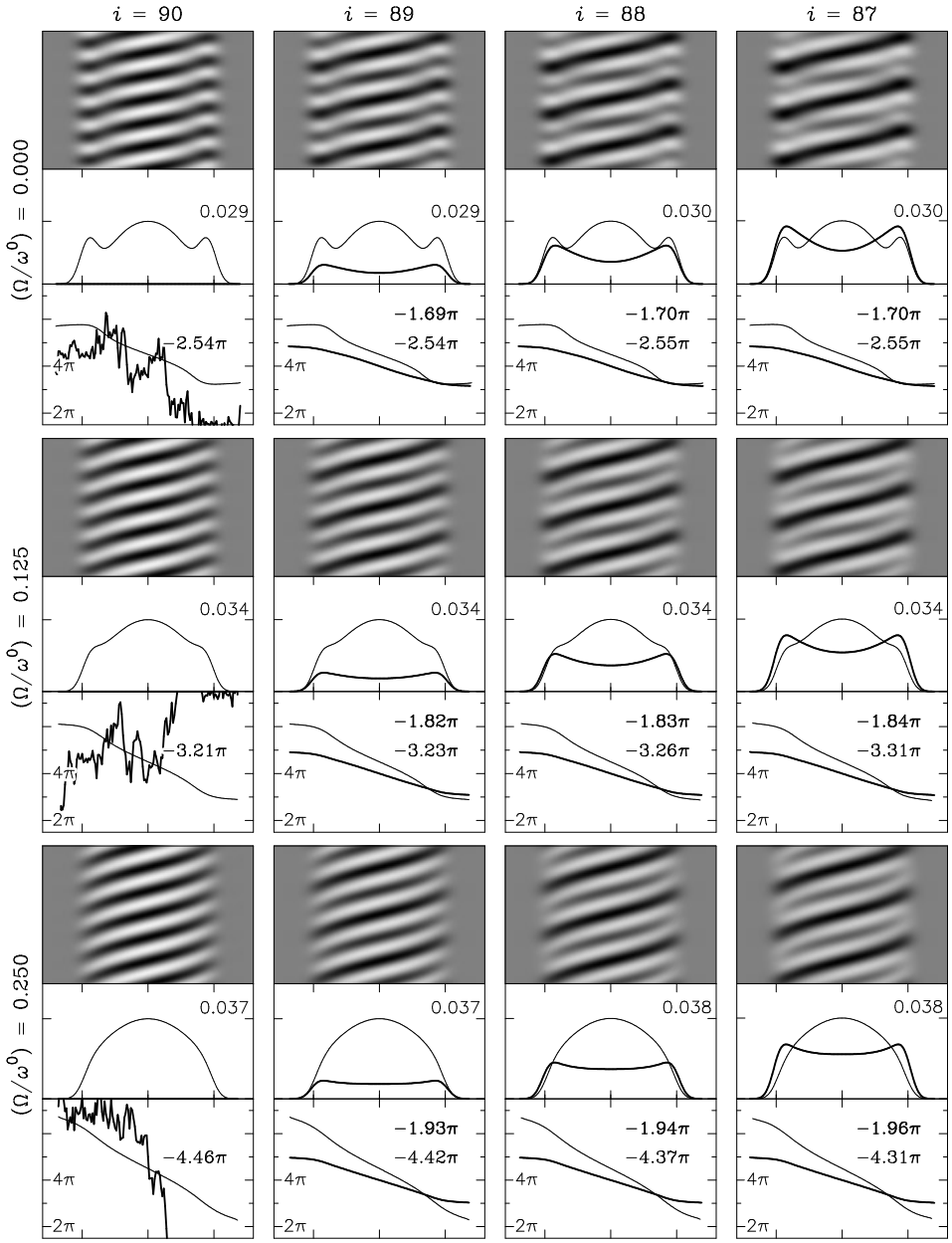

Fig. 3. Line-profile variations due to a non-radial pulsation mode with ℓ=2 m=−1, as a function of inclination angle i and rotation parameter $\Omega/\omega^{(0)}$. See Fig. 1 for the other relevant parameters. The amplitude and phase diagrams are all plotted on the same scale. Note that for i=90° the amplitude of the variations with the pulsation frequency ($I_0(\lambda)$, thick lines) is zero throughout the line profile and that consequently the corresponding phase diagram ($\Psi_0(\lambda)$, thick lines) is undefined. This is the case for both the zero-rotation model ($\Omega/\omega^{(0)}$=0) and the slow-rotation model ($\Omega/\omega^{(0)}>0$)

i=85°, $V_e \sin i$=100 km/s, intrinsic line width W=15 km/s, rotation parameter $\Omega/\omega^{(0)}$=0.25. In the bottom right part of the figure the amplitudes of the variations of the first (thick curve) and second (thin) velocity moments are given, expressed in units of $V_e \sin i$ and $(V_e \sin i)^2$ respectively. In the left part of the figure the amplitude and phase diagrams of the intensity variations are drawn. For each wavelength/velocity bin in the profile we fitted the normalized intensity $I(\lambda, t)$ with a combination of sinusoids with frequencies that are multiples of the input (observed) pulsation frequency

$$I(\lambda,t) = I_{\rm mean}(\lambda) + I_0(\lambda)\sin(\omega_{\rm obs}t + \Psi_0(\lambda)) + I_1(\lambda)\sin(2\omega_{\rm obs}t + \Psi_1(\lambda)) + I_2(\lambda)\sin(3\omega_{\rm obs}t + \Psi_2(\lambda)) \quad . \tag{3}$$

In the figures we plot the amplitude and phase distributions of the line-profile variations with frequency equal to the pulsation frequency $I_0(\lambda)$, $\Psi_0(\lambda)$ and its first harmonic $I_1(\lambda)$, $\Psi_1(\lambda)$ as a function of wavelength.

From Fig. 1 we see that, as expected (Paper II), the absolute phase difference of the line-profile variations with the pulsation frequency, when expressed in π radians, is close to the input value of the degree ℓ of the dominant pulsation mode.

4. The effects of inclination and rotation on line profiles of non-radially pulsating stars

In Fig. 2 we present our computations with the same input parameters as used for Fig. 1, except for the inclination which we set equal to 90°. We find that in the exact equator-on

case the number of bumps in the profiles doubles (see also Kambe & Osaki 1988), which is equivalent to an increase of the relative importance of the harmonic amplitudes.

Furthermore, we see that the variation in the first velocity moment (i.e. centroid velocity) vanishes, and that the second moment shows variations with twice the pulsation frequency. These features in the moment variations are typical for modes with an odd value for $\ell-m$ that are seen from an equator-on perspective. This is the reason why identification of ℓ, m and i with the moment method is straightforward for these cases. However, for pulsation modes with $\ell\gtrsim4$ the variations in the first few moments are very small and hard to detect with present day observing techniques, and hence the moment method can only be used for low-degree modes.

In Fig. 3 we display our model calculations for different values of inclination and the rotation parameter $\Omega/\omega^{(0)}$. The other relevant input parameters are the same as those used for the time series in Figs. 1 and 2. The top row of panels in Fig. 3 shows the result of our calculations with a zero-rotation model.

Note that we show three full pulsation cycles in the grey-scale diagrams, without explicitly specifying the time scales on the vertical axes. This way the pulsation frequencies appear to be constant in our diagrams (Figs. 3 and 4), even though we vary $\Omega/\omega^{(0)}$. The horizontal axes are scaled to $V_{\rm e}\sin i$.

Inclination

In Figs. 2 and 3 we see that the amplitudes of the line-profile variations are rather low, which is the result of cancellation effects. In the equator-on case all line-profile variations leading to asymmetry of the line profile cancel out, since for an ℓ=2 $|m|$=1 spheroidal mode the motions at the top half of the stellar disc are opposite to the motions at the bottom half. However, these motions still give rise to changes in line width, which occur with a frequency of twice the pulsation frequency, i.e. the first harmonic.

The fact that the line width varies can be understood by considering the integration of a blue and a red-shifted profile, either of them originating from the top or the bottom half of the equator-on stellar disc. The summation of these profiles results in a less-deep and broader line profile than in the case of no oscillatory motions. Since in the integrated stellar light the observer cannot distinguish between top and bottom, the line-width changes appear with mainly the first harmonic of the pulsation frequency.

Increasing the inclination to the equator-on situation one expects a decrease of variations occurring with the input frequency, resulting in vanishing amplitudes for i=90°. Since the phases are undefined for zero amplitudes the phase diagram $\Psi_0(\lambda)$ of the variations with the input pulsation frequency gives no information at all for i=90°. This is evident in both the rotating and non-rotating case.

We see that for inclination angles slightly different from i=90° one expects to observe a continuous phase relation with a maximum blue-to-red phase difference $\Delta\Psi_0$ that is not significantly different for all investigated values of the inclination. The change in inclination hardly affects the harmonic amplitude and phase distributions $I_1(\lambda)$ and $\Psi_1(\lambda)$.

Rotation

As evidenced by the time series of residual spectra in Fig. 3 the line-profile characteristics of the ℓ=2, m=−1 mode are hardly qualitatively changed by the effects of rotation. The amplitude distribution $I_0(\lambda)$ of the variations with input pulsation frequency is similar for all investigated rotation values. The same holds for the slope of the phase distribution $\Psi_0(\lambda)$. In Fig. 3 we see that the extra terms in the eigenfunction due to the Coriolis force give rise to an increase of the harmonic amplitude and a steepening of the harmonic phase diagram. We want to stress however, that for a different choice of stellar and pulsational parameters these effects can be less evident or different (Paper I).

For the investigated spheroidal mode, the two toroidal terms that are due to the Coriolis force have pulsation parameters ℓ=1, m=−1 and ℓ=3, m=−1. These particular toroidal motions also have the equatorial plane as plane of symmetry of the oscillatory motions, and therefore the line-profile variations with the pulsation frequency are also cancelled out in the case of a rotating star ($\Omega/\omega^{(0)}>0$) with i=90°.

From a mode as considered here (and by Reid & Aerts), an observer can detect line-profile variations with the pulsation frequency with a blue-to-red phase difference of $\Delta\Psi_0\sim-2\pi$, except if i=90°. In Paper II we showed that the absolute blue-to-red phase difference $\Delta\Psi_0$ (of the variations appearing with the pulsation frequency) is a direct measure of the degree ℓ of the pulsation, and that the harmonic phase difference $\Delta\Psi_1$ puts constraints on the value of $|m|$:

$$\ell \;\approx\; -0.10 + 1.10|\Delta\Psi_0|/\pi \qquad (4)$$

$$|m| \;\approx\; -1.10 + 0.61|\Delta\Psi_1|/\pi\ . \qquad (5)$$

For these equations we used the coefficients that are valid for modes with low values of k (see Paper II for other subsets of parameter space).

From Fig. 3 and Eq. (4) we find that for $i\neq$90° the derived phase difference $\Delta\Psi_0$ is in agreement with what is expected within the limits of the model of adiabatic oscillations corrected for first-order rotation effects. Therefore we do not expect an erroneous identification of the degree of the mode if the inclination angle is different from the exact equator-on situation.

The IPS method is intrinsically weak in identifying low values of $|m|$ (see Paper II), especially in the case of large values of the rotation parameter $\Omega/\omega^{(0)}$. With the values of $\Delta\Psi_1$ in Fig. 3 and with Eq. (5), we find that for the investigated mode $|m|$ will be overestimated as $|m|$=2 , in the cases when the Coriolis force is important.

5. Moving bumps in the Be star η Cen

As an application of our findings we consider the results reported by Leister et al. (1994), who find blue-to-red moving bumps in absorption lines of the Be star η Cen. They show that at any

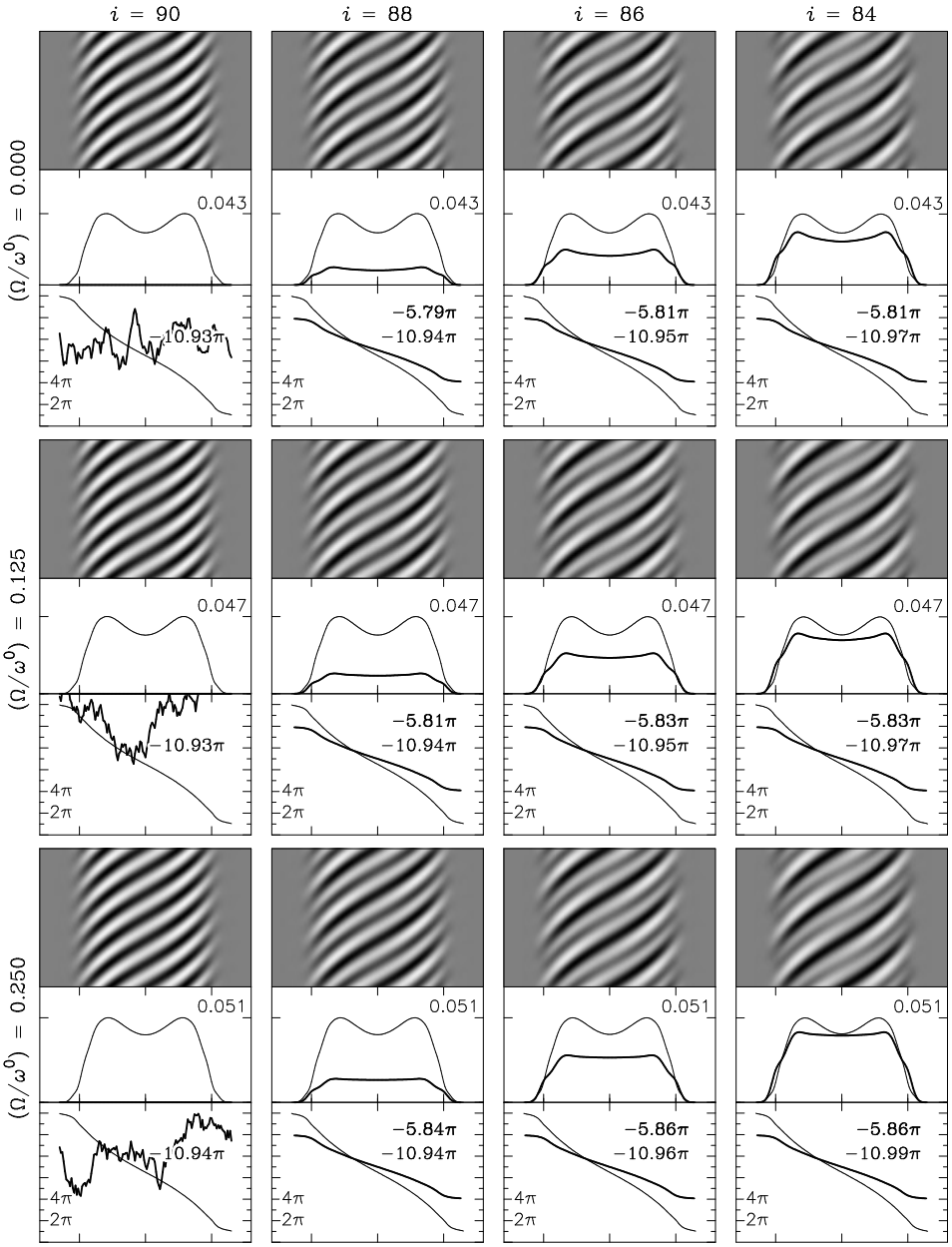

Fig. 4. Line-profile variations due to a non-radial pulsation mode with ℓ=7 m=−6, as a function of inclination angle i and rotation parameter $\Omega/\omega^{(0)}$. We used W=0.1$V_{\rm e}$ sin i, $V_{\rm max}$=0.1$V_{\rm e}$ sin i and $k^{(0)}$=0.25. Note that the number of bumps in the spectra is only doubled for a very limited range of the inclination angle

instant at least 6 bumps are visible in the profile, and attribute these to the presence of a sectoral non-radial pulsation mode with ℓ=14±4. Inspired by the work of Kambe & Osaki (1988), Leister et al. mention the possibility that the bumps can also be due to a tesseral mode with ℓ=7 and $|m|$=6. Here we argue that the observer can discriminate between these possibilities from an accurate frequency analysis.

In Fig. 4 we plot line-profile variations of a pulsation mode with ℓ=7 and m=−6. We see from the figure that the effects of the Coriolis terms are not as important as for low degree modes. From the phase differences $\Delta\Psi_0$ and $\Delta\Psi_1$ in this figure and Eqs. (4) and (5) we find that in principle both ℓ and $|m|$ can be retrieved for this mode, within the accuracy discussed in Paper II.

As in Fig. 3, we see that only close to the equator-on situation the number of bumps is actually doubled. The bumps can only be misinterpreted as due to a mode with ℓ=14 for a small range in inclination where the variational amplitude $I_0(\lambda)$ is too small to be detected. For inclination angles smaller than i=90° we see a pattern of subsequent deep and less-deep bumps, with the less-deep bumps gradually disappearing for even smaller inclination angles.

For near equator-on cases a tesseral mode with $\ell-|m|$=1 characterizes itself by large harmonic amplitude $I_1(\lambda)$ in comparison with $I_0(\lambda)$, and can therefore be distinguished from a near equator-on sectoral mode by an evaluation of the variations found at these frequencies. For sectoral modes the harmonic amplitude $I_1(\lambda)$ is always smaller than $I_0(\lambda)$, independent of the inclination.

Hence, if the apparent frequency of the bumps in η Cen is the actual pulsation frequency, then the profile variations can be due to a ℓ=14 pulsation mode. If the main apparent frequency is the harmonic of the actual pulsation frequency, then the profile variations are due to a mode with ℓ=7 and m=−6. In the latter case the real pulsation frequency should be detectable as well, except if the inclination angle is exactly i=90°.

6. Conclusions

We have shown that for a non-radial pulsation with ℓ=2, $|m|$=1 and i=90°, cancellation effects cause all line-profile variability with the pulsation frequency to disappear. The fact that in this situation the remaining line-profile variability with the first harmonic of the pulsation frequency can mimic that of a higher degree/order mode, is entirely due to these cancellation effects (caused by the precise equator-on value of the inclination), and is not due to effects of rotation. For the same reason, the variability of the first velocity moment of this mode vanishes for i=90°. Furthermore, for this mode the evaluation of the phase diagram of the intensity variations with the pulsation frequency is of little physical relevance, since the phases are not defined for zero amplitudes. For an inclination angle only slightly different from 90°, the pulsation does give rise to variations with the pulsation frequency. The corresponding phase diagram practically does not change for any other investigated value of the inclination. Therefore we recommend, for test studies of observable line-profile characteristics of tesseral modes, not to generate spectra using an inclination angle exactly equal to 90°.

Tesseral modes with a nodal line on the equator ($\ell-|m|$ an odd number) are the only modes for which this extreme cancellation effect for i=90° can be expected. The other case of perfect cancellation of any line-profile variation with the pulsation frequency, is the pole-on situation for modes with $m\neq0$. However, in this case the phase diagrams resulting from the IPS method will in practice be not of any use, since the line profiles are not rotationally broadened. Therefore we conclude that the conclusion of Reid & Aerts (1993) on the restricted applicability of the method of evaluating the phase diagram (IPS method), only applies to the exact equator-on case. Even for i=89°.5 the IPS method gives the expected results. Given the number of stars suitable for an IPS analysis, we expect that in practice the number of cases for which line-profile variations of a possible mode with $\ell-|m|$=1 would be misinterpreted, is very small. Nevertheless, we encourage observers also to make use of the information that is held in the velocity moments of the absorption line profiles. Especially for low degree modes the first few velocity moments give very useful information.

We have argued that one should be able to investigate whether the line-profile variations in the Be star η Cen are due to a sectoral pulsation mode with ℓ=14 or due to a tesseral mode with ℓ=7, $|m|$=6. In the latter case one expects to find an alternating pattern of deep and less-deep bumps, if the inclination angle is not exactly i=90°. In this case one expects to detect both the apparent pulsation frequency and its first harmonic with an IPS analysis. The variational power found at the first harmonic should be larger or of the same order as that found at the pulsation frequency itself. From the phase diagram of the variations at the pulsation frequency one can derive the degree ℓ of the mode.

Acknowledgements. We thank Huib Henrichs and Jan van Paradijs for discussions, many helpful suggestions and careful reading of the manuscript. We especially thank Conny Aerts for her many constructive remarks and the antwerp-style rolls.

This research is supported by the Netherlands Foundation for Research in Astronomy (NFRA) with financial aid from the Netherlands Organization for Scientific Research (NWO), under project 781-71-043 (JHT).

References

Aerts, C., de Pauw, M., Waelkens, C. 1992, A&A, 266, 294
Aerts, C., Waelkens, C. 1993, A&A, 273, 135
Baade, D. 1984, A&A, 135, 101
Balona, L.A. 1986, MNRAS, 219, 111
Clement, M.J. 1994, in: Pulsation, rotation and mass loss in early type stars, Proc. IAU Symp. 162, ed. L. Balona, H.F. Henrichs and J.-M. Le Contel, Kluwer
Floquet, M., Hubert, A.M., Janot-Pacheco, E., Mekkas, A., Hubert, H., Leister, N.V. 1992, A&A, 264, 177
Gies, D.R., Kullavanijaya, A. 1988, ApJ, 326, 813
Henrichs, H.F. 1991, in: Rapid Variability of OB stars, ESO Conference and Workshop Proc. 36, p. 199
Kambe, E., Osaki, Y. 1988, PASJ, 40, 313
Kambe, E., Ando, H., Hirata, R. 1990, PASJ, 42, 687
Kennelly, E.J., Walker, G.A.H., Merryfield, W.J. 1992, ApJ, 400, L71
Lee, U., Jeffery, C.S., Saio, H. 1992, MNRAS, 254, 185
Leister, N., Janot-Pacheco, E., Hubert, A., Floquet, M., Hubert, H., Briot, D. 1994, A&A, 287, 789
Martens, L., Smeyers, P. 1982, A&A, 106, 317
Martens, L., Smeyers, P. 1986, A&A, 155, 211
Mathias, P., Aerts, C., De Pauw, M., Gillet, D., Waelkens, C. 1994 A&A, 283, 813
Reid, A.H.N., Aerts, C. 1993, A&A, 279, L25
Reid, A.H.N., Bolton, C.T., Crowe, R.A., Fieldus, M.S., Fullerton, A.W., Gies, D.R., Howarth, I.D., McDavid, D., Prinja, R.K., Smith, K.C. 1993, ApJ, 417, 320
Saio, H. 1981, ApJ, 244, 299
Schrijvers, C., Telting, J.H., Aerts, C., Ruymaekers, E. 1996, (Paper I) in press (A&A Suppl. Series)
Smith, M.A. 1978, ApJ, 224, 927
Telting, J.H., Schrijvers, C. 1996, (Paper II) in press (A&A)
Vogt, S.S., Penrod, G.D. 1983, ApJ 275, 661

This article was processed by the author using Springer-Verlag LaTeX A&A style file *L-AA* version 3.